HHS Public Access

Author manuscript

*Phys Chem Chem Phys*. Author manuscript; available in PMC 2019 July 18.

Published in final edited form as:

*Phys Chem Chem Phys*. 2018 July 18; 20(28): 19030–19036. doi:10.1039/c8cp03842b.

# Defining the Conditional Basis of Silicon Phthalocyanine Near-IR Ligand Exchange

**Erin D. Anderson**[†], **Stacey Sova**[‡], **Joseph Ivanic**[§], **Lisa Kelly**[‡], and **Martin J. Schnermann**[†,*]

[†]Chemical Biology Laboratory, Center for Cancer Research, National Cancer Institute at Frederick, Frederick, USA

[‡]Department of Chemistry and Biochemistry, University of Maryland, Baltimore County, 1000 Hilltop Circle, Baltimore, Maryland 21250, United States

[§]Advanced Biomedical Computational Science Group, Frederick National Laboratory for Cancer Research operated by Leidos Biomedical Research, Inc., Frederick, Maryland 21702, United States

## Abstract

Bond cleavage reactions initiated by long-wavelength light are needed to extend the scope of the caged-uncaged paradigm into complex physiological settings. Axially unsymmetrical silicon phthalocyanines (SiPcs) undergo efficient release of phenol ligands in a reaction contingent on three factors - near-IR light (690 nm), hypoxia, and a thiol reductant. These studies detail efforts to define the mechanistic basis for this unique conditionally-dependent bond cleavage reaction. Spectroscopic studies provide evidence for the formation of a key phthalocyanine radical anion intermediate formed from the triplet state in a reductant-dependent manner. Computational chemistry studies indicate that phenol ligand solvolysis proceeds through a heptacoordinate silicon transition state and that this solvolytic process is favored following SiPc radical anion formation. These results provide insight regarding the central role that radical anion intermediates formed through photoinduced electron transfer with biological reductants can play in long-wavelength uncaging reactions.

## Graphical Abstract

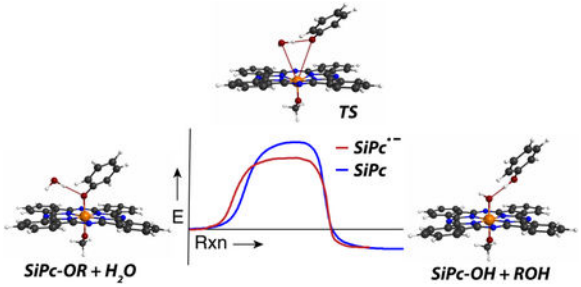


*martin.schnermann@nih.gov

Conflicts of Interest

There are no conflicts to declare.

## Introduction

Photochemical reactions that release, or “uncage”, payload molecules have applications in diverse fields.[1] Near-IR light has favorable properties for biological use, including meaningful tissue transmittance and low toxicity. However, the identification of chemical reactions initiated by these wavelengths is a significant chemical challenge.[2] Recent progress has provided some of the first biologically useful options in this area. The underlying mechanism that leads to bond cleavage varies widely. Several methods rely on the local generation of singlet oxygen ($^1O_2$), which then mediates bond cleavage.[3-6] Photocleavage of various metal-heteroatom bonds has been explored extensively, with significant progress achieved using various ruthenium and cobalamin complexes.[7-8] Finally, there has been exciting recent progress using certain common organic chromophores (e.g. BODIPY).[9-11]

Conventional photodynamic therapy (PDT) methods exhibit diminished utility in hypoxic conditions. Consequently, uncaging reactions useful for drug delivery that are initiated selectively by long-wavelength light and hypoxia would have certain benefits.[12] Recently, we developed a near-IR uncaging reaction involving axially unsymmetrical, water soluble silicon phthalocyanines (SiPcs) that occurs in physiologically relevant hypoxic conditions.[13] SiPcs have been studied extensively for their efficient $^1O_2$-generating properties, and have progressed to clinical trials as photodynamic therapy agents.[14-16] In addition to their photosensitizing properties, SiPcs have also been reported to undergo other photochemical reactions with potential utility for uncaging applications. Studies by Burda and coworkers have shown that SiPcs with axial alkyl ligands (bond dissociation energy (BDE) ≈ 40 kcal/mol) undergo efficient cleavage with 690 nm irradiation.[17] Our work demonstrated that the Si-OAr bond (BDE ≈ 80 kcal/mol) of axially unsymmetrical SiPcs can be cleaved with near-IR light in an aqueous environment, while exhibiting excellent dark stability.[13] This bond cleavage process is dramatically accelerated by the presence of a thiol reductant (present in mM concentrations in an intracellular environment) and low $O_2$ conditions.[13] We demonstrated that the biological activity of these molecules depends on $O_2$-tension (Figure 1). Specifically, under normoxic conditions, SiPcs effectively generate reactive oxygen species (ROS) with ROS-dependent inhibition of cell growth. By contrast, under low $O_2$ conditions, these compounds undergo axial-ligand exchange, leading to drug-dependent effects on cell growth.[13]

With a specific interest in defining the conditional basis of the uncaging process, here we report a mechanistic analysis of the axial Si-OAr bond cleavage reaction. Using compound **1** (Figure 1A) as a model substrate, we have carried out a series of spectroscopic and computational analyses. These studies provide strong evidence for the general reaction model shown in Figure 1B. In this pathway, a radical anion intermediate formed through photoinduced electron transfer (PET) from the SiPc triplet state undergoes solvolytic ligand exchange. Laser flash photolysis enables characterization of the SiPc triplet and its reductant-dependent conversion to the SiPc radical anion. Spectroscopic characterization of the radical anion suggests its role as the key intermediate in the bond cleavage process. Computational chemistry studies indicate that the ligand exchange reaction involves a heptacoordinate silicon transition state and that this solvolytic process is favored following

SiPc radical anion formation. Insight into these mechanistic features will enable the design of SiPc caging groups with improved properties.

## Results

Our first goal in these studies was to interrogate the initial intermediates formed following irradiation. In our prior study, we hypothesized that radical anion formation (which was estimated to have a half-life of 45 sec)[13] proceeds from the SiPc triplet state. To examine this issue further, we employ laser flash photolysis spectroscopy. Shown in Figure 2A is the $T_1$-$T_n$ absorption spectrum of SiPcUmb (**1**, Figure 1A) in argon-saturated pH 7.4 PBS at 510 nm. The lifetime of $T_1$ was found to be 120 μs. These data indicate that the triplet state is formed with an estimated quantum yield of 0.036 (± 0.003) (Figure S1 and S2). This value is somewhat lower than that observed with other SiPcs.[18] This lower value may reflect excited state quenching by the pendent umbelliferone ligand (see Figures S3 and S4 for further discussion).

We then examined the glutathione (GSH)-mediated formation of the radical anion from this triplet intermediate. We previously demonstrated that radical anion formation is quenched in the presence of oxygen and that no fluorescence quenching occurs with high concentrations of GSH (16 mM).[13] While these observations are consistent with the intermediacy of a triplet state, electron transfer processes are known to happen on both the SiPc excited singlet state and the SiPc excited triplet state.[19-20] The long-lived SiPc triplet observed above was quenched by GSH (≤ 5 mM) with a bimolecular rate constant of $3.23 \pm 0.22 \times 10^6$ $M^{-1}s^{-1}$ (Figure 2B). Additionally, the transient absorption spectrum of **1** with GSH in deoxygenated PBS show a transient species that absorbs at 580 nm that persists after the triplet-state has decayed (inset of Figure 2C). We assign this long-lived species as the radical anion of **1**, consistent with transient and steady-state absorption spectra of other SiPc radical anions.[21-23] These results provide strong evidence that a radical anion intermediate is generated in an aqueous environment through a PET-mediated process.

Having demonstrated that the radical anion can be efficiently generated in a reductant-dependent manner, we sought to further characterize the axial-ligand exchange reaction. During initial photorelease studies, we observed spectroscopic changes that were dependent on irradiation with near-IR light, the inclusion of a reductant (GSH), and the exclusion of oxygen. Specifically, a solution of **1** in deoxygenated PBS containing 5 mM GSH was estimated to have a photodegradation quantum yield ($\Phi_{PD}$) of 0.0027, roughly 900-fold greater than in PBS alone without deoxygenation.[13] We also found that the reaction proceeds to high chemical conversion for uncaging (71%), although tracking the identity of SiPc products and the oxidized thiol product has proven challenging. Here, we investigate this reaction further with intermittent irradiation experiments (Figure 3). Brief irradiation (1 min, 25 $mW/cm^2$, 690 nm) of a deoxygenated solution of SiPc **1** (25 μM) and 5 mM glutathione leads to loss of the parent SiPc Q-band at 690 nm (Figure 3B). Also upon irradiation, a sharp increase in absorbance at 585 nm, diagnostic for the SiPc radical anion, is observed (Figure 3B).[20, 24] Dark incubation after irradiation leads to partial recovery of the parent 690-nm signal and disappearance the $SiPc^{\bullet -}$ 585-nm peak. The fluorescence reporter 4-methyl umbelliferone is not fluorescent when attached to the SiPc core but

becomes so upon release. Monitoring 4-methyl umbelliferone fluorescence under identical conditions leads to light-dependent increases upon irradiation (Figure 3C).

An alternative pathway to Si-O bond cleavage might entail energy transfer from the excited Pc macrocycle, in either the singlet or triplet state, to the Si-O bond and bond cleavage.[25] As the radical anion hydrolysis pathway is a putatively a light independent process, we sought to generate this species through ground state chemistry and then assess the axial ligand exchange reaction. To generate the radical anion intermediate independently, we examined the impact of stronger reductants without irradiation in the presence and absence of $O_2$. Following a small screen of reductants, ligand exchange of **1** can be initiated with tris(2-carboxyethyl)phosphine (TCEP) (1 mM), a stronger reductant than GSH (oxidation potential for TCEP = −0.29 V vs. −0.16 V for GSH),[26] without irradiation (Figure 4). Ligand release under these conditions was highly oxygen dependent, as seen in the photochemical reaction. This observation is in line with our previous studies, in which we demonstrated that $O_2$ is an efficient quencher of the SiPc radical anion.[13] Collectively, these studies support the notion that axial ligand cleavage follows SiPc radical anion formation through a purely solvolytic ground state pathway. Additionally, this data suggests that likely both the triplet state and the radical anion play a key role in establishing the $O_2$-sensitive nature of the photochemical ligand exchange reaction.

The studies above provide significant insight regarding key intermediates, particularly the radical anion species, in route to axial ligand exchange. A still outstanding question in our mind was the basis of the enhanced reactivity of the radical anion to solvolytic displacement. To address this issue, we turned to computational analysis. In these studies, quantum chemistry calculations at the B3LYP-PCM/6-31G(d) level of theory were performed (see Methods); note that the Polarized Continuum Model (PCM) aims to account for solvent effects, in this case water. The model neutral SiPc(OMe)(OPh) and radical anion $SiPc^{\bullet-}$(OMe)(OPh) systems have been investigated, where OMe and OPh represent analogs of the actual 1,3-bis(trimethylaminium)-2-propanol (with $2I^-$ counterions) and 4-methylumbelliferone ligands used in the experiments, respectively. We first contrasted the properties of the aforementioned neutral and radical anion molecules by determining their propensities for OMe and OPh ligand exchange. We hypothesize that these processes occur via hydrolytic reactions. Although the Si-OH products have not been isolated in our studies, such species are known to be insoluble and prone to aggregation.[27-28] Direct Si-O bond homolysis, observed with the Si-C bond of SiPcs[25] is not feasible due to the significantly higher bond strength of the Si-O bond (~80 kcal vs ~40 kcal for Si-C bond).[29] More specifically, we determined the energy barriers that must be overcome to replace OPh and OMe with OH, i.e., energetics for the competing reactions of neutral SiPc(OMe)(OPh)--$H_2O$ to form the products Si(OH)(OPh)--HOMe vs. Si(OMe)(OH)--HOPh, and analogously for the radical anion species. The computed energy profiles for the four reactions are shown in Figure 5A, where transition states (having exactly one imaginary frequency) were mapped to their corresponding reactants/products via intrinsic reaction coordinate (IRC) computations (see Methods). For the neutral SiPc(OMe)(OPh) system, we found that uncaging of OMe entails overcoming a significantly higher barrier (53.8 kcal/mol, solid red line) than that required to uncage OPh (35.2 kcal/mol, solid blue line). However, for the radical anion

$SiPc^{\bullet -}$ (OMe)(OPh) species, the OMe and OPh replacement barriers are reduced to 48.5 kcal/mol (dashed red line) and 29.0 kcal/mol (dashed blue line), respectively.

Figure 5 shows computed structures of reactants, transition states, and products describing the radical anion OMe (Figure 2B) and OPh (Figure 2C) uncaging processes. Of note, the corresponding structures for neutral uncaging reactions are very similar (see Supporting Information). It is clear that OMe uncaging barriers are by far the highest, and thus unlikely to occur for either neutral or radical anion states. In contrast, OPh replacement energy barriers are significantly smaller, with that for the radical anion (29.0 kcal/mol) lying 6.2 kcal/mol lower than for the neutral species (35.2 kcal/mol). This energy difference implies that OPh uncaging occurs some 35,000 times faster for the radical anion state vs. neutral (via Arrhenius rate equation using T=298 K and equivalent collision coefficients). In addition, the barrier for the reverse reaction, OPh replacing OH, for the radical anion is 8.1 kcal/mol higher than the forward, ensuring that the OPh uncaging reaction is essentially irreversible. Thus, the behavior of the SiPc can be rationalized as follows: (i) OMe (representing 1,3-bis(trimethylaminium)-2-propanol (with $2I^-$ counterions)) ligand exchange energy barriers are far too high to occur for either neutral or radical anion species, (ii) the barrier height for OPh (representing 4-methylumbelliferone) ligand exchange is slightly too high to occur spontaneously in the neutral state, (iii) upon formation of the radical anion, either by irradiation in the presence of glutathione or by the addition of a stronger reductant like TCEP, the OPh release barrier is lowered enough so that it happens at a noticeable rate, and (iv) the OPh uncaging process is irreversible since the product complex is computed to be more stable than the reactant by some 8 kcal/mol. Of note, the heptacoordinate silicon transition state indicated by these studies have been suggested elsewhere in nucleophilic substitutions on hexacoordinate silicon atoms.[30-33]

In an effort to understand why the OPh uncaging barrier is lowered upon reduction, we investigated the properties of neutral and radical anion SiPc(OMe)(OPh). The optimized structure of the radical anion is illustrated in Figure 6. The neutral system is very similar, the only real difference being the angle of the methyl group (See Supporting Information). Also shown are the Si–O bond lengths (which are reasonably similar, lying between 1.73 and 1.79 Å) and Mulliken charges, where it is clearly noted that these properties remain relatively unchanged when going from neutral to the reduced state. Of interest is that the substantial silicon positive charge (+1.1 $e^-$) is almost exactly opposite the sum of the oxygen negative charges (−0.5 $e^-$ and −0.6 $e^-$ for O(Me) and O(Ph), respectively) for both neutral and radical anion systems, indicating that the captured electron is situated entirely on the phthalocyanine ligand. This is visually confirmed via illustration of the highest occupied molecular orbital (alpha spin), i.e., the radical orbital, shown in Figure 6. As such, although the nature of the Si–O bonds appear relatively unchanged upon reduction, it is likely that the resultant increased electrostatic repulsions between the negatively charged phthalocyanine ligand and oxygen atoms give rise to lower energy barriers for OMe and OPh removal, with that for the latter being low enough to be spontaneous and irreversible at room temperature.

## Conclusions

SiPics represent a promising scaffold for light-mediated treatment and drug delivery. An unusual feature of the axial ligand exchange reaction is the requirement of 3 conditions; near-IR light, the presence of a reductant and low oxygen tension. These provide significant insight regarding the likely pathway to ligand exchange, which involves a critical SiPc radical anion intermediate. Spectroscopic studies demonstrate that the SiPc excited triplet state is the immediate precursor for SiPc radical anion formation. We have confirmed the clear role of the thiol reductant in initiating light-mediated ligand uncaging. Finally, the demonstration of ligand release from the ground state Pc radical anion, generated without irradiation, lends support to its role as the critical intermediate in the ligand exchange process. Computational studies indicate that nucleophilic attack of water on the SiPc Si center is more favorable for the SiPc radical anion than for the parent compound. These studies delineate the requirements for the conditional release of a phenol payload from the SiPc macrocycle and inform efforts to design new SiPc and other long-wavelength uncaging systems. Additionally, the potential for uncaging reactions involving a central role for a radical anion intermediate, generated through the combined action of long-wavelength light and biologically-abundant reductants, has been validated through these efforts and may be now reasonable to consider with other molecular scaffolds.

## Methods.

### Reagents.

All commercially obtained reagents were used as received. Tris(2-carboxyethyl)phosphine (TCEP), glutathione (GSH), and pH 7.4, 50 mM phosphate buffered saline (PBS) were obtained from Sigma-Aldrich. Compound **1** was synthesized as reported previously.[13]

### Flash Photolysis.

Nanosecond transient absorption studies were carried out using the technique of laser flash photolysis. Pulsed excitation at 355 nm (ca. 50 mJ/pulse) was provided by the third harmonic of a Q-switched Nd-YAG laser. Solutions of SiPcUmb(**1**) (2 μM in pH 7.4, 50 mM PBS) were prepared in quartz cuvette. The system has been previously described.[34] All solutions were argon purged unless otherwise indicated.

### Triplet Quantum Yield.

The triplet quantum yield of **1** was determined by comparative actinometry using a benzophenone standard.[35] A value of 0.036 ± 0.003 was obtained as follows. Solutions of **1** (in PBS) and benzophenone (in acetonitrile) were prepared with matched 355-nm optical densities ($OD_{355}$ = 0.300) and subjected to laser excitation. The triplet quantum yield ($\phi_T^{SiPc1}$) of **1** was determined using eq (1)

$$\phi_T^{SiPc1} = \frac{\Delta A_{520}^{SiPc1}}{\Delta A_{520}^{BP}} \frac{\Delta \varepsilon_{520}^{BP}}{\Delta \varepsilon_{520}^{SiPc1}} \phi_T^{BP} \quad (1)$$

Where $\frac{\Delta A_{520}^{SiPc1}}{\Delta A_{520}^{BP}}$ is taken as the slope of the plot of the $T_1$-$T_n$ absorption change for **1** vs. BP (0.115 ± 0.005) (Figure S1). The $T_1$-$T_n$ extinction coefficient ($\Delta\varepsilon_{520}^{BP} = 6500 \pm 400\,M^{-1}cm^{-1}$), along with an intersystem crossing yield ($\phi_T^{BP}$) of 1.0 were used for the benzophenone standard. [36]

The triplet-triplet extinction coefficient for **1** in aqueous phosphate buffer was determined from a plot of the magnitude of triplet-triplet absorption vs. ground-state bleach (Figure S2). A value of 20800 ± 1000 $M^{-1}cm^{-1}$ was obtained for $\Delta\varepsilon_{520}^{SiPc1}$ from the slope of the plot (−0.224 ± 0.011), along with the known ground-state extinction coefficient at 690 nm (93000 $M^{-1}cm^{-1}$).[13]

## Intermittent Irradiation.

Irradiations were performed with a 690-nm LED illuminator, mounted on a heatsink with lens (set is sold together as L690-66-60-550, Marubeni, Inc.) and powered by an EPS-600 Mini-Power Supply (C.B.S. Scientific Company, Inc.). Samples were irradiated with 25 mW $cm^{-2}$ of 690-nm light and light intensity measurements were performed with a Thorlabs PM200 optical power and energy meter fitted with a S120VC standard Si photodiode power sensor (200-1100 nm, 50 mW). Samples were irradiated in quartz cuvettes with septum screw caps. Samples were deoxygenated by bubbling Ar (balloon) through the septum cap of the sealed cuvette. Cuvettes were equipped with stir bars and stirred for the duration of the experiment. Fluorescence traces were recorded on a PTI QuantaMaster steady-state spectrofluorometer operated by FelixGX 4.0.3 software with 2 nm excitation and emission slit widths and 0.1 s integration rate. Samples were excited at 360 nm and emission recorded at 445 nm to evaluate 4-methylumbelliferone fluorescence. Absorbance traces were taken on a Shimadzu UV-2550 spectrophotometer operated by UVProbe 2.32 software.

## Quantum chemistry.

The computations in this study were executed using the GAMESS[37-38] package and molecular structures and orbitals were illustrated using MacMolPlt.[39] We have used the density functional theory (DFT)[40] method with the B3LYP[41-42] hybrid density functional (containing VWN5 functional).[43] Restricted Hartree-Fock (RHF)[44] references were used for closed-shell (neutral) molecules while restricted open-shell Hartree-Fock (ROHF)[45] references were used for radical anion (negatively charged) systems. The double-zeta 6-31G(d) basis sets were used throughout[46-48] and water solvent effects were treated using the Polarizable Continuum Model (PCM)[49-52] (with a high density of tesserae: NTSALL = 960 in $PCM) where in some cases an explicit quantum mechanical water molecule was included within the PCM model. Geometries were optimized to tight convergence criteria (maximum Cartesian gradient < $10^{-5}$ Hartree/Bohr) using analytic gradients and Hessians were computed seminumerically (double differences) using analytic gradients for all stationary points located. Minimum energy paths connecting transition states and corresponding reactant/product minima were determined using the second-order intrinsic reaction coordinate (IRC) method of Gonzalez and Schlegel.[53] Atomic charges were

determined using Mulliken's population analysis.[54] Structures and electronic energies of all stationary points described are given in the Supporting Information.

## Supplementary Material

Refer to Web version on PubMed Central for supplementary material.

## Acknowledgements

This work was supported by the Intramural Research Program of the National Institutes of Health, National Cancer Institute, Center for Cancer Research. This work was supported with federal funds from the National Cancer Institute, National Institutes of Health, under Contract No. HHSN 261200800001E (for J.I.). The content of this publication does not necessarily reflect the views or policies of the Department of Health and Human Services.

## References.

1. Lee HM, Larson DR and Lawrence DS, ACS Chem. Biol, 2009, 4, 409. [PubMed: 19298086]
2. Solomek T, Wirz J and Klan P, Acc. Chem. Res, 2015, 48, 3064. [PubMed: 26569596]
3. Nani RR, Gorka AP, Nagaya T, Kobayashi H and Schnermann MJ, Angew. Chem, 2015, 54, 13635. [PubMed: 26403799]
4. Nani RR, Gorka AP, Nagaya T, Yamamoto T, Ivanic J, Kobayashi H, and Schnermann MJ, ACS Central Sci., 2017, 3, 329.
5. Gorka AP, Nani RR, Zhu J, Mackem S and Schnermann MJ, J. Am. Chem. Soc, 2014, 136, 14153. [PubMed: 25211609]
6. Bio M, Rajaputra P, Nkepang G and Youngjae Y, J. Med. Chem, 2014, 57, 3401. [PubMed: 24694092]
7. Shell TA and Lawrence DS, Acc. Chem. Res, 2015, 48, 2866. [PubMed: 26479305]
8. Knoll JD, Albani BA and Turro C, Acc. Chem. Res, 2015, 48, 2280. [PubMed: 26186416]
9. Slanina T, Shrestha P, Palao E, Kand D, Peterson JA, Dutton AS, Rubinstein N, Weinstain R, Winter A, and Klan P, J. Am. Chem. Soc, 2017, 139, 15168. [PubMed: 29039200]
10. Goswani PP, Syed A, Beck CL, Albright TR, Mahoney KM, Unash R, Smith EA, and Winter AH, J. Am. Chem. Soc, 2015, 137, 3783. [PubMed: 25751156]
11. Paleo E, Slanina T, Muchova L, Solomek T, Vitek L, and Klan P, J. Am. Chem. Soc, 2016, 138, 126. [PubMed: 26697725]
12. Karimi M, Sahandi Zangabad P, Baghaee-Ravari S, Ghazadeh M, Mirshekari H, and Hamblin MR, J. Am. Chem. Soc, 2017, 139, 4584. [PubMed: 28192672]
13. Anderson ED, Gorka AP, and Schnermann MJ, Nat. Commun, 2016, 7, 13378. [PubMed: 27853134]
14. He J, Larkin HE, Li YS, Rihter D, Zaidi SJ, Rodgers MA, Mukhtar H, Kenney ME, and Oleinick NL, Photochem. Photobiol, 1997, 65, 581. [PubMed: 9077144]
15. Allen CM, Sharman WM, Van Lier JE, J. Porphyrins and Phthalocyanines, 2001, 5, 161.
16. Mitsunaga M, Ogawa M, Kosaka N, Rosenblum LT, Choyke PL and Kobayashi H, Nat. Med, 2011, 17, 1685. [PubMed: 22057348]
17. Cheng Y, Doane TL, Chuang CH, Ziady A and Burda C, Small, 2014, 10, 1799. [PubMed: 24515950]
18. Nyokong T, Coord. Chem. Rev, 2007, 251, 1707.
19. Darwent JR, Douglas P, Harriman A, Porter G and Richoux M-C, Coord. Chem. Rev, 1982, 44, 83.
20. Uslan C, Oppelt KT, Reith LM, Sesalan BS, and Knor G, Chem. Commun, 2013, 49, 8108.
21. Zhang X-F and Wang J, J. Phys. Chem. A, 2011, 115, 8597. [PubMed: 21744830]
22. Oldham TC and Phillips D, J. Phys. Chem. B, 1999, 103, 9333.
23. Doane TL, Chuang CH, Chomas A and Burda C, Chemphyschem, 2013, 14, 321. [PubMed: 23307629]

24. Daziano JP, Steenken S, Chabannon C, Mannoni P, Chanon M and Julliard M, Photochem. Photobiol, 1996, 64, 712. [PubMed: 8863479]
25. Doane T, Cheng Y, Sodhi N and Burda C, J. Phys. Chem. A, 2014, 118, 10587. [PubMed: 25153643]
26. Peng L, Xu X, Guo M, Yan X, Wang S, Gao S, and Zhu S, Metalllomics, 2013, 5, 920.
27. Maree MD, Kuznetsova N and Nyokong T, J. Photochem. Photobiol. A, 2001, 140, 117.
28. Doane T, Choma A, Srinivasan S and Burda C, Chem. Eur. J, 2014, 20, 8030. [PubMed: 24861009]
29. Li J, Yang Y, Zhang P, Sounik J and Kenney ME, Photochem. Photobiol. Sci, 2014, 13, 1690. [PubMed: 25308695]
30. Kano N, Nakagawa N and Kawashima T, Angew. Chem, 2001, 40, 3450. [PubMed: 11592167]
31. Kameo H, Kawamoto T, Sakaki S, Bourissou D and Nakazawa H, Organometallics, 2014, 33, 6557.
32. Carre F, Chuit C, Corriu RJP, Fanta A, Mehdi A and Reye C, Organometallics, 1995, 14, 194.
33. Carre F, Chuit C, Corriu RJP and Reye C, New J. Chem, 1992, 16, 63.
34. Rogers JE and Kelly LA, J. Am. Chem. Soc, 1999, 121, 3854.
35. Carmichael I and Hug GL, J. Phys. Chem. Ref. Data, 1986, 15, 1.
36. Bensasson RV and Gramain JC, J. Chem. Soc. Faraday Trans. 1, 1980, 76, 1801.
37. Schmidt MW, Baldridge KK, Boatz JA, Elbert ST, Gordon MS, Jensen JH, Koseki S, Matsunaga N, Nguyen KA, Su S, Windus TL, Dupuis M and Montgomery JA, J. Comput. Chem, 1993, 14, 1347.
38. Gordon MS and Schmidt MW, Theory Appl. Comput. Chem.: First Forty Years, 2005, 1167.
39. Bode BM and Gordon MS, J. Mol. Graph. Model, 1998, 16, 133. [PubMed: 10434252]
40. Kohn W and Sham LJ, Phys. Rev, 1965, 140, 1133.
41. Becke AD, J. Chem. Phys, 1993, 98, 5648.
42. Stephens PJ, Devlin FJ, Chabalowski CF and Frisch MJ, J. Phys. Chem, 1994, 98, 11623.
43. Hertwig RH and Koch W, Chem. Phys. Lett, 1997, 268, 345.
44. Roothaan CCJ, Rev. Mod. Phys, 1951, 23, 69.
45. Roothaan CCJ, Rev. Mod. Phys, 1960, 32, 179.
46. Hehre WJ, Ditchfield R and Pople JA, J. Chem. Phys, 1972, 56, 2257.
47. Harihara PC and Pople JA, Theor. Chim. Acta, 1973, 28, 213.
48. Gordon MS, Chem. Phys. Lett, 1980, 76, 163.
49. Li H and Jensen JH, J. Comput. Chem, 2004, 25, 1449. [PubMed: 15224389]
50. Li H, J. Chem. Phys, 2009, 131, 184103. [PubMed: 19916594]
51. Tomasi J, Mennucci B and Cammi R, Chem. Rev, 2005, 105, 2999. [PubMed: 16092826]
52. Miertus S, Scrocco E and Tomasi J, Chem. Phys, 1981, 55, 117.
53. Gonzalez C and Schlegel HB, J. Chem. Phys, 1989, 90, 2154.
54. Mulliken RS, J. Chem. Phys, 1955, 23, 1833.

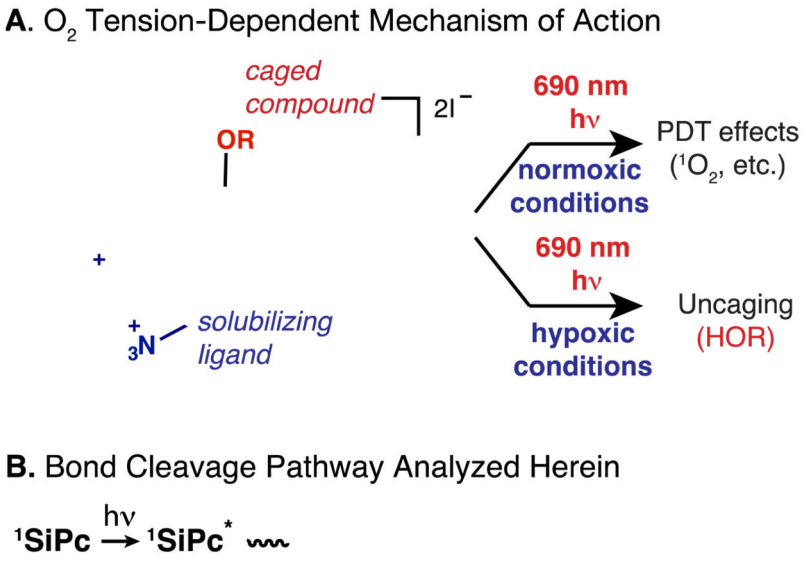


**Fig 1.**

$O_2$ Tension-dependent mechanism of action (**A**) and general bond cleavage pathway analyzed in these studies (**B**).

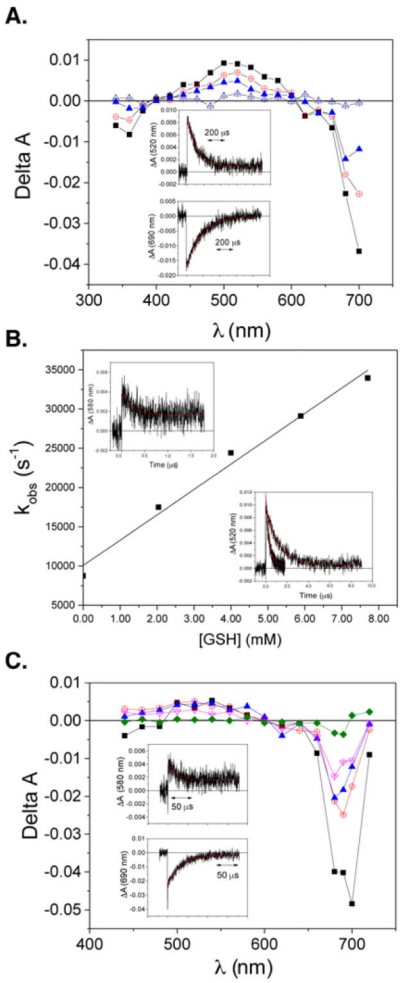


**Fig 2.**

(A) Transient absorption spectra obtained after 355-nm pulsed excitation of SiPcUmb **(1)** in argon-saturated PBS (0, 45, 109 and 526 μs in order of decreasing ΔA). Insets depict decay kinetics at 520 and 690 nm (with superimposed single-exponential fit). (B) Bimolecular quenching plot for quenching of the $T_1$ state of SiPc-Umb by GSH (in argon-saturated PBS). (C) Transient absorption spectra obtained after 355-nm pulsed excitation of SiPc-Umb in argon-saturated PBS containing 10.1 mM GSH. Times shown are 0, 2, 11.4, 22.4 and 109 μs after the laser pulse (in order of decreasing ΔA). Insets depict decay kinetics at 580 and 690 nm (with superimposed single-exponential fit).

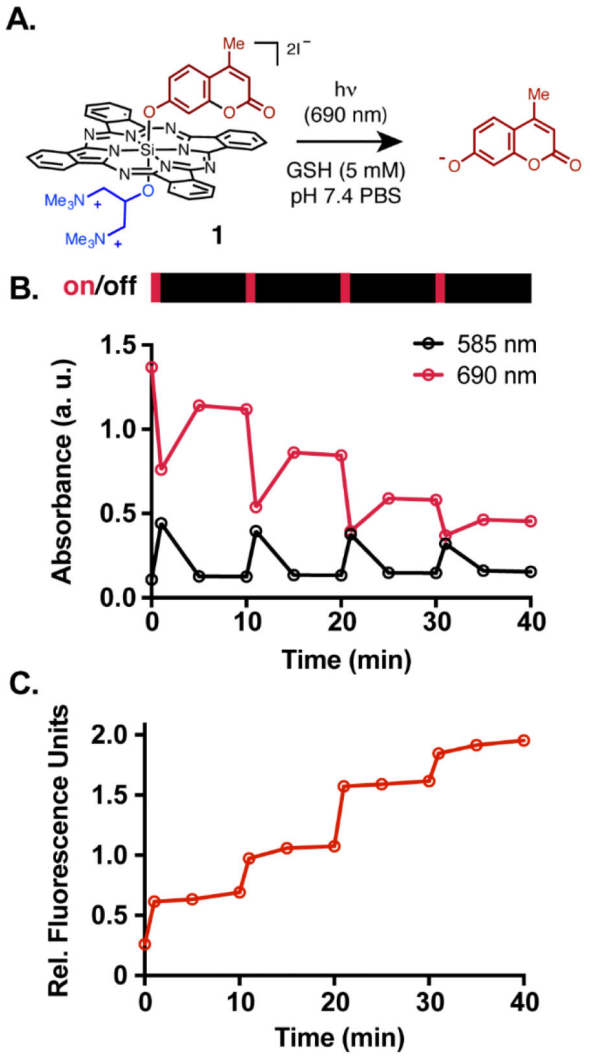


**Fig 3.**

Intermittent irradiation of compound **1**. (A) General scheme of uncaging reaction. (B) Absorbance at 690 nm (red) and at 585 nm (black) and (C) Umbelliferone fluorescence at 445 nm of deoxygenated 25 μM solutions of **1** (pH 7.4 PBS with 5 mM GSH) for 4 cycles of intermittent irradiation (1 min, 25 mW $cm^{-2}$, 690 nm irradiation; 9 min dark).

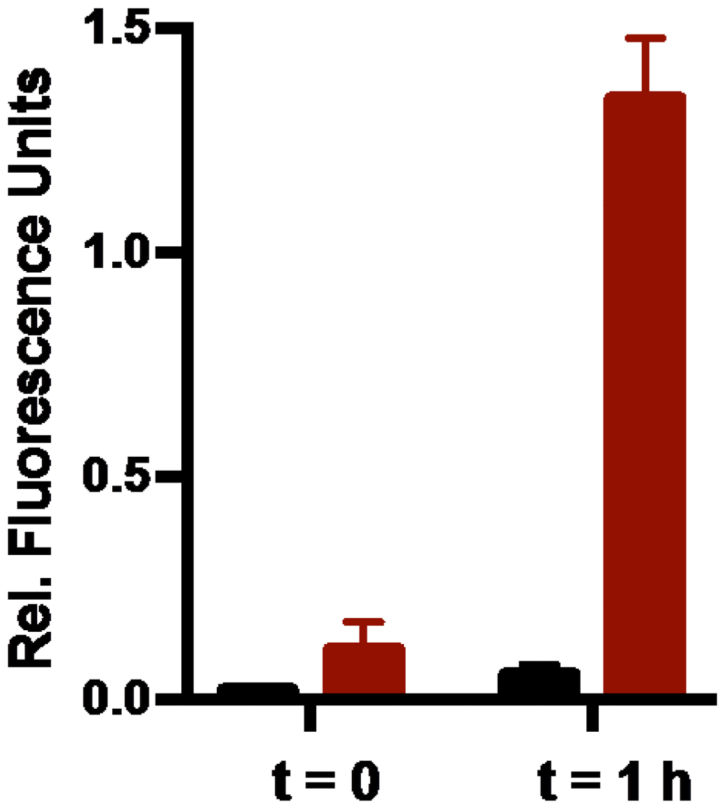


**Fig 4.**

Fluorescence intensity at 445 nm of 25 μM solutions of **1** (PBS (50 mM, pH 7.5)) with 1 mM TCEP with no deoxygenation (black) and deoxygenation (red) at 0 and 1 h of stirring in the dark.

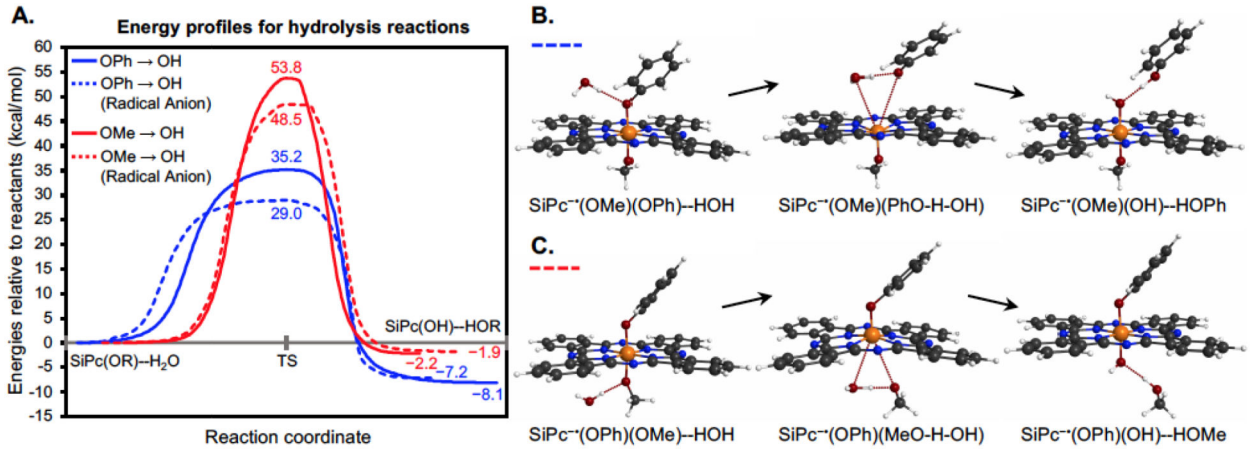


**Fig 5.**

(A) Energetics of the possible hydrolysis reactions of neutral and anionic SiPc(OPh)(OMe) systems leading to displacements of HOPh and HOMe. Transition state barriers are decreased when going from neutral (solid lines) to radical anion (dashed lines) where HOPh release for the latter is most favored and likely spontaneous. Note that the reverse reaction (HOPh displacing $H_2O$) is highly improbable due to the notably larger barrier of 37.1 kcal/mol. (B & C) Structures of reactants, transition states, and products for hydrolysis reactions of anionic SiPc(OPh)(OMe) leading to (B) HOPh and (C) HOMe displacements; structures for neutral reactions are very similar (see Supporting Information).

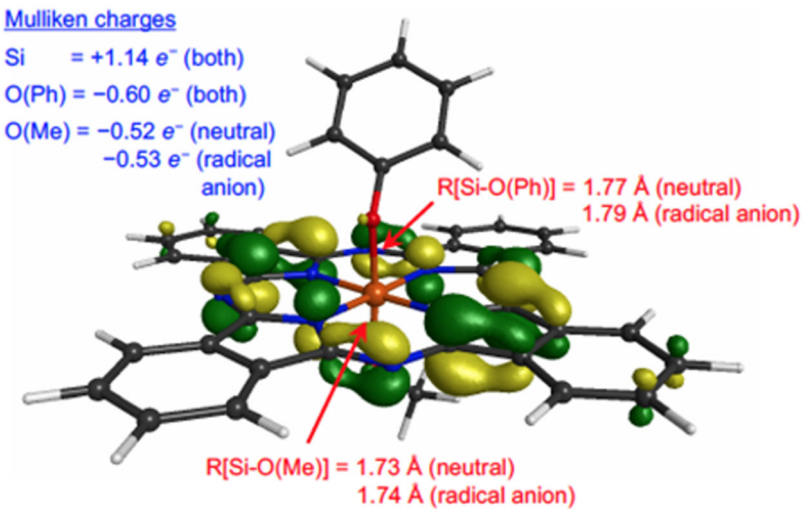


**Fig 6.**

Illustrations of the structure of the anionic SiPc(OMe)(OPh) system and the radical molecular orbital (alpha spin HOMO); the geometry of the neutral system is very similar (see Supporting Information). Also shown are Mulliken charges of the silicon and oxygen atoms (blue text) and Si–O bond lengths (red text) for both neutral and anionic states.